

Morphological Characteristic Evaluation of Road Aggregates

Subjects: [Engineering, Civil](#) | [Construction & Building Technology](#)

Contributor: Jue Li , Lei Wang , Yongsheng Yao , Yiyang Tao , Kefei Liu

The sustainable performance of asphalt pavement depends on the quality and mix design of road aggregates. Identifying aggregate morphology and size is a prerequisite step for material design and numerical modeling of asphalt mixtures.

aggregate

morphology

asphalt mixture

mechanical property

shape

angularity

texture

1. Introduction

Asphalt mixtures are used in over 90% of highway construction in China. Currently, asphalt pavement generally has a short service life, and there is a gap in the design life. Aggregates account for more than 90% of the total mass of asphalt mixtures. Mineral aggregate, a vitally important road material, forms a good load-bearing capacity after gradation combination and sufficient compaction and can be used directly in the paving of the subgrade or subbase of road structures ^[1]. At the same time, multiphase composites are structurally characterized by a coarse aggregate skeleton and fine aggregate filling through binders such as asphalt and cement ^[2]. These materials have long dominated the pavement structure. Using aggregate properties to improve their mixes' mechanical properties and service life has been an important area of research in road engineering.

2. Morphological Characteristic Evaluation

The engineering properties of road materials (e.g., asphalt mixes and cement concrete) are influenced by the morphological characteristics (shape, angle, and texture) of the aggregates ^[3]. Therefore, suitable evaluation methods and indicators can better quantify the morphological characteristics of aggregates. Specifically, the shape profile and angularity of coarse aggregates belong to the macroscopic category, while the surface texture belongs to the microscopic category ^[4]. The relationship among shape, angularity and surface texture is shown in **Figure 1**.

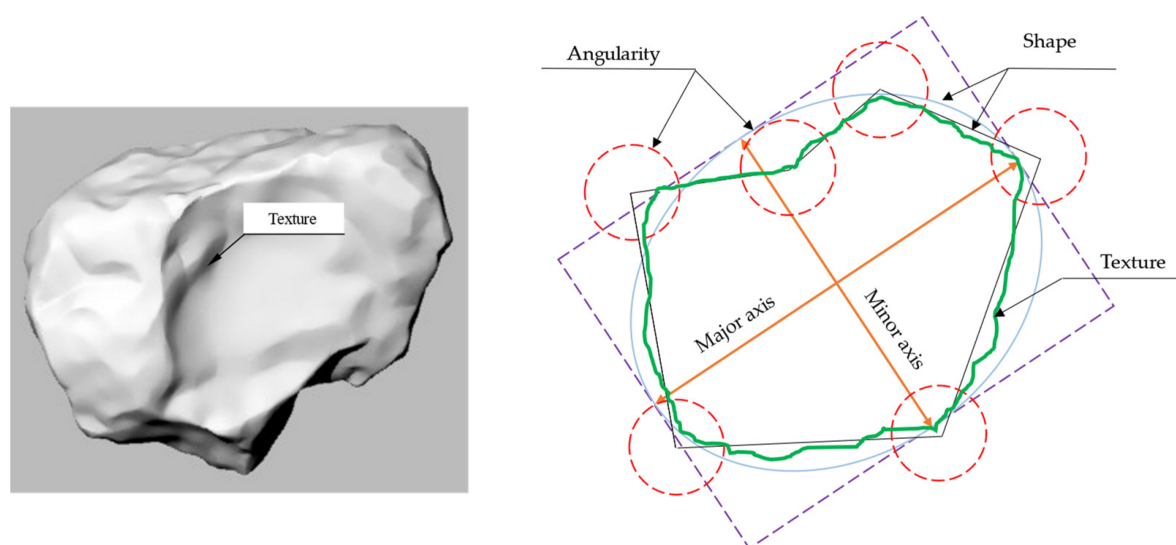


Figure 1. Relationship among shape, angularity and surface texture.

2.1. Shape

The shape of the aggregate can be divided into two dimensions and three dimensions, and the analysis of the aggregate shape can be divided into sphericity and shape factor, roundness, formation index, Fourier series, flat length ratio, aspect ratio, width ratio, symmetry, and three-dimensional shape factor [5]. As for the contour characteristics of particles, the concept of two-dimensional planes is mainly involved. With the development of digital image technology, the quantitative indexes of contour shape have progressed from shallow to deep, from the simple fine length to the development of relatively fine angular roundness. The fine length, also known as the axis ratio, is generally defined as the ratio of the long axis to the short axis of the equivalent ellipse of the planar projection of the aggregate.

The indicators characterizing the shape of the aggregates can be distinguished into 2D and 3D. Among them, most of the 2D metrics use length and area for shape characterization, such as form index (2D), roundness, the ratio of breadth to width, etc. It is easy to lose a lot of shape detail information. The aggregates' shape, angularity and texture are effectively separated by the Fourier series method. Three-dimensional indexes include shape factor (SF), flat and elongated ratio (FER), and sphericity (ψ). These indexes can characterize the aggregate morphology more accurately. The shape index of aggregate with calculation equations and main characteristics is shown in Table 1.

Table 1. Shape index of aggregate with calculation equations and main characteristics.

| Shape Indexes | Equations * | Characteristics | Literatures |
|-----------------|--|--|-------------|
| Form index (2D) | $\sum 360 - \Delta\theta = 0 R\theta + \Delta\theta - R\theta R\theta$ | Quantifying the 2D image of fine aggregates of relative form and using incremental changes in the particle radius. | [6] |

| Shape Indexes | Equations * | Characteristics | Literatures |
|--|---|--|-------------|
| Aspect ratio (AR) | D_{max}/D_{min} | These parameters use the length and area method to characterize the shape of the aggregate; however, it loses a large amount of shape detail information | [7] |
| Rectangular degree (RD) | AAMER | | [8] |
| Axial coefficient (AC) | L_{max}/L_{min} | | [9] |
| Eccentricity (E) | ca | Eccentricity could characterize the shape of the aggregate particles and reflect the elliptical oblate degree. | [7] |
| Roundness | $4\pi AL^2$ | Roundness was the inverse of the form factor. In early imaging techniques, it was used to calculate 2D features of particle shape. | [10] |
| Form index using Fourier series (FRFORM) | $R(\theta) = a_0 + \sum_{m=1}^{\infty} [a_m \cos(m\theta) + b_m \sin(m\theta)]$ | Fourier series can be used to analyze the form, angularity, and texture of aggregate shape. | [11] |
| Form (shape) index (Fourier series) | $12 \sum_{m=1}^m [(a_m a_0)^2 + (b_m a_0)^2]$ | | [11] |
| Ratio of Breadth to Width | $\min(x_c) / \max(x_{Fe})$ | Breadth to width ratio can be used to describe the form of aggregate particles. | [12] |
| Symmetry | $12[1 + \min(r_1 r_2)]$ | Symmetry is a term that some imaging systems use to describe aggregate form. | [12] |
| Shape Factor (SF) | $DSDL \times Di / V$ | Shape Factor was a typical index in a system that represented in terms of three dimensions (longest, intermediate, and shortest dimensions). | [13] |
| Flat and elongated ratio (FER) | DLDS | FER represents the ratio between the longest dimension and the shortest dimension of a particle. | [14] |
| Sphericity (ψ) | $DS \times Di / DL^2 \sqrt{3}$ | Sphericity is a 3D parameter, which can characterize the | [15] |

Mora et al. [16] proposed a method for measuring the sphericity, shape factor and convexity of concrete aggregates, which estimated the thickness and volume of the particles, measured the thickness-dependent shape parameters,

| Shape Indexes | Equations * | Characteristics | Literatures |
|--|-------------|---------------------------------------|---------------|
| [17] | | aggregate morphology more accurately. | Rousan et al. |
| [18] | | | nba et al. |
| <p>reconstructed a three-dimensional model of aggregate particles after obtaining data from three-dimensional laser scans of various types of aggregates. This laser scanning technique can better quantify the morphological characteristics of aggregates by calculating the sphericity from surface area and volume, the sphericity from three orthogonal dimensions, and the flat-length ratio from the longest and shortest dimensions of the aggregate profile; θ—directional angle; $\Delta\theta$—incremental difference in the angles; R_θ—radius of the particle at angle θ; $R_{\theta+\Delta\theta}$—radius of the particle at angle $\theta+\Delta\theta$; D_{\max}—the maximum length of the minimum external rectangle of the aggregate profile; D_{\min}—minimum size of the minimum external rectangle; A—Area of the aggregate profile; $AMER$—area of minimum circumscribed rectangle. L_{\max}—major axis length of equivalent ellipse; L_{\min}—minor axis length of equivalent ellipse. c—focal length of ellipse with same second moment; a—major axis of the ellipse. The brittleness index is an important shape parameter in aggregates widely used in infrastructure construction, such as roads, and Anochie-Boateng et al. [19] developed a new equation for the brittleness index and verified its threshold frequencies separating shape and angularity. x_c—maximum chord; x_{Fe}—the Feret diameter. r_1, r_2—the reliability. Laser scanning technology provided more accurate evaluation results and improved the selection of distances of the center of gravity to the edge in a given direction. DL—length, longest dimension; DI—width, intermediate dimension, the maximum dimension in the plane perpendicular to the length; DS—thickness, shortest surface characteristics of crushed and uncrushed aggregates in asphalt mixtures using the 3D laser scanning technique, which had a good correlation with the experimental results. Ge et al. [22] proposed the flatness elongation index, sphericity index and specific surface area to characterize various aspects of the morphological characteristics of coarse aggregates and derived that small-size aggregates have a larger proportion of elongated particle number.</p> | | | |

From the above research, it can be seen that the 3D scanning technique can well-characterize the aggregate's shape. However, previous studies using 3D scanning technology have mainly focused on the shape, volume, and surface properties of aggregates from one or different quarries, with less research on the morphological decay pattern of aggregates during application.

2.2. Angularity

Aggregate angularity essentially describes the degree of sharpness of the angles. Corner roundness was proposed by Wadell [23] and others to describe the sharpness of the combination of corners and edges of a particle and was generally considered to be related to the radius of curvature or geometric fractal of the particle profile at the sharp end, while for quantitative evaluation, most researches have used the method of fitting similar polygons to obtain the angularity parameter of an aggregate. Fractals were first created by Mandelbrot [24] and have been widely used in various disciplines through continuous development. Fractals are used as a theoretical tool to describe and evaluate some characteristics such as hierarchical continuity, irregularity or randomness [25], and asphalt mixtures exhibit statistical self-similarity in volume and properties, which is suitable for quantitative analysis with fractal theory.

Wang et al. [26] proposed a unified Fourier morphological analysis method to quantify the shape characteristics of aggregates. Zhang et al. [27] proposed an index to characterize the combined effect of rib angle and surface texture of coarse aggregates, i.e., AT, and investigated the statistical distribution pattern of the AT index for different grain sizes of basalt aggregates and their composite aggregates. Rajan et al. [28] studied the comparison of rib angles of

different grain sizes of aggregates under different crusher production. The angularity index of aggregate with calculation equations and main characteristics is shown in **Table 2**.

Table 2. Angularity index of aggregate with calculation equations and main characteristics.

| Angularity Indexes | Equations * | Characteristics | Literatures |
|---------------------------------|--|---|-------------|
| Angularity | $12\sum_{m=1}^n 1 + m^2 [(a_m a_0)^2 + (b_m a_0)^2]$ | Fourier series analysis was applied to measure the angularity of aggregate in PIAS. | [26] |
| Angularity factor (AF) | $AF = \sum_{p=1}^N \sum_{q=1}^N [(a(p,q)a_0)^2 + (b(p,q)a_0)^2]$ | The fast Fourier transform method could be applied to calculate and analyze the angularity factor (AF) of aggregate in FTI. | [29] |
| Surface erosion-dilation method | $A1 - A2A1 \times 100\%$ | As a popular image processing technique, erosion dilation was utilized to analyze the angularity of aggregate particles in the UIAIA. | [30] |
| Gradient angularity (GA) | $1n3 - 1\sum_{i=1}^n 3 \theta_i - \theta_{i+3} $ | Higher values of GA indicate more angular aggregate particles. | [31] |
| Angularity index (AI) (radius) | $\sum_{\theta=0}^{\theta=360} \Delta\theta Rp\theta - REE\theta / REE\theta$ | As the defining equation of angularity. | [15] |
| 3D angularity (3DA) | $13\sum_{i=1}^n Pti \cdot AtiPte \sum_{i=1}^n Ati + \sum_{i=1}^n nrPri \cdot AriPre \sum_{i=1}^n nrAri + \sum_{i=1}^n nfPfi \cdot AfiPfe \sum_{i=1}^n nfAfi$ | 3D parameters for more accurate characterization | [31] |

| Angularity Indexes | Equations * | Characteristics | Literatures |
|--------------------------------|---|---|-------------|
| [35] | | of aggregate morphology. | |
| Angularity parameter | $(pconvexpellipse)^2$ | All of them optimize the profile of the particles of the aggregate but cannot retain the original morphological characteristics of the aggregate. | [32] |
| Convexity | $A_{particle}/A_{convex}$ | | [33] |
| Average angularity coefficient | $I = \sum_{i=1}^n P_i \times a_i / 100$ | | [34] |

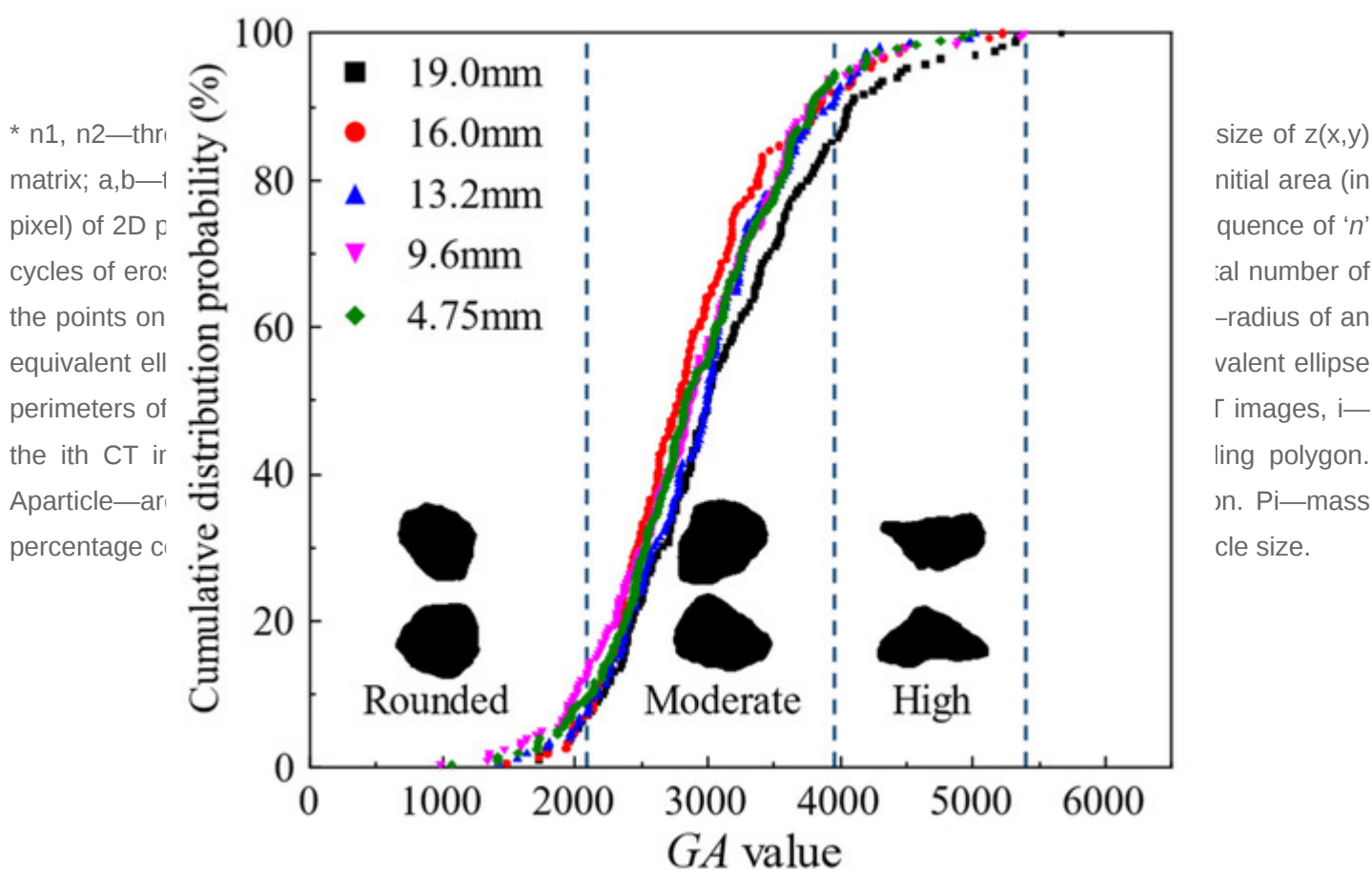


Figure 2. Distribution of GA values for aggregates.

Zhu et al. [36] collected the aggregate characteristics by a 3D blue-ray scanner, and evaluated the effect of coarse aggregate size and angles on the volumetric properties of asphalt mixtures. Huang et al. [37] prepared mixes with similar aggregate gradation using five different angular levels of coarse-grained aggregates and three different asphalt binders and evaluated the coarse aggregate angles (CAA) by compacted voids in coarse aggregates (VCA) and triaxial shear tests.

In summary, researchers have proposed various evaluation indicators to further improve the road performance of road aggregates from different angles by studying the angularity of aggregates. Currently, many shape indices

have been proposed by mathematical methods. However, most of the studies of these indices are based on graphical and statistical laws. Their correlation with the mechanical properties of aggregates lacks research. At the same time, the applicability of these indices for the prediction of the structural properties of the mixture still lacks a uniform classification standard.

2.3. Texture

The aggregate texture is mainly distinguished by the smoothness and roughness of aggregate particles. Miller et al. [38] proposed an analytical method to describe the surface texture of asphalt pavements using laser profiles to estimate friction characteristics. Al-Assi et al. [39] used Close-Range Photogrammetry (CRP) to measure the changes in micro texture on asphalt pavements. Khasawneh et al. [40] proposed an equation based on nonlinear regression to calculate the texture of asphalt pavements and the steady state's texture features. Du et al. [41] utilized a 2D wavelet method to describe the texture obtained by a 3D laser scanner on asphalt pavement. Hu et al. [42] conducted an analysis of the influence of texture on the skid resistance of asphalt pavements by using the collected pavement surface texture data. The texture index of aggregate with calculation equations and main characteristics is shown in **Table 3**.

Table 3. Texture index of aggregate with calculation equations and main characteristics.

| Texture Indexes | Equations * | Characteristics | Literatures |
|--|--|--|-------------|
| Texture factor (TF) | $\sum_{p=1}^N \sum_{q=1}^N [(a(p,q)a_0)^2 + (b(p,q)a_0)^2] - AF$ | Fast measurement of aggregated morphological features based on 2D fast Fourier transform. | [43] |
| Texture index (TI) | $13N \sum_{i=1}^3 \sum_{j=1}^N (D_{i,j}(x,y))^2$ | Quantization of textures using wavelet methods. | [43] |
| Erosion dilation area ratio (EDR) | $A1 - A2A1 \times 100\%$ | Changes in area after erosion and dilatation cycles are directly related to aggregate texture. | [44] |
| Comprehensive erosion dilation area ratio (CEDR) | $\sum_{i=1}^n (a_i \times EDR_i) \sum_{i=1}^n a_i$ | Aggregate gradation is considered. | [45] |
| Surface texture | $\sum_{m=3}^n m = n^2 + 1 a m^2 + b m^2 - \dots - \sqrt{\quad}$ | The shape, angularity and texture of the aggregates are considered separately. | [26] |
| Fourier series analysis method | $12 \sum_{m=n^2+1}^{\infty} [(a m a_0)^2 + (b m a_0)^2]$ | Calculation of the surface fabric of aggregates used in PIAS. | [11] |
| Direct measurement of | $(PP_{convex})^2$ | For evaluating textures, the texture parameters are | [32] |

| Texture Indexes | Equations * | Characteristics | Literatures |
|-------------------------------------|--|--|-------------|
| aggregate dimensions | | related to the perimeter. | |
| Three-dimensional Texture (MT3DSHF) | $MT3D = \sum_{n=26} n \max \sum_{m=-1}^n a_{nm} $ $MT3DN = MT3Da00$ | 3D textures can be calculated. Can differentiate between aggregates with similar sizes. Used to compare aggregates of different sizes and volumes. | [46] |

All asphalt mixture is a typical nonhomogeneous composite material consisting of irregularly shaped and distributed aggregates, asphalt binder and voids [47][48]. The aggregate morphological characteristics significantly influence the properties of asphalt mixtures [49][50], which can be found in existing studies. Improving the performance of asphalt mixes based on morphological characteristics of aggregates accounting for 90% of the total erosion and expansion is an important research direction. Traditional methods of testing aggregate morphological characteristics are time-consuming and rely heavily on subjective judgments, resulting in imprecise experimental results. In most of the tests, it is difficult for the researchers to control the aggregate morphological characteristics

variables [51]. Aragão et al. [52] mixed aggregates from different sources and tested them using AIMS to obtain aggregates with different angles and textures; nevertheless, it was impossible to distinguish which morphological characteristics were responsible for the effect. Wang et al. [53] employed a modified Los Angeles (LA) wear test to obtain aggregates with different angles, calculated the fractal dimension and changed the size and surface texture of the aggregates. Puzzo et al. [54] proposed a 3D model evaluation method for pavement texture based on digital image processing techniques, which used photographs to generate a Digital Surface Model (DSM) to calculate the digital Mean Texture Depth (MTD) and calculate and analyze other texture parameters for contour extraction.

Cui [43] evaluated the effect of aggregate morphology variation on the performance of asphalt pavements and investigated the asphalt coverage ratio and the mechanical properties of the mixture for different types of aggregates to quantify the aggregate morphological characteristics by AIMS. An accurate definition of the aggregate morphological characteristics is important for the initial design phase of pavements, extending the service life of roads and reducing the use of natural aggregates and the generation of solid waste.

Inadequate adhesion between asphalt and aggregate can cause severe distress in pavement structure and service life [55], and the conventional approach, which does not consider active adhesion mechanisms, is hardly convincing. Cui et al. [56] investigated and designed an active adhesion-based test method to compensate for the adhesion deficiency and used digital image processing techniques to quantify the adhesive properties. The results showed that digital image processing could measure the asphalt coating ratio accurately and effectively.

In summary, the texture is a micro-morphological characteristic of the aggregate. The greater the complexity of the surface texture, the greater the internal friction angle that can be generated when the aggregates are embedded and locked with each other after crushing. Aggregate texture has fewer means of characterization relative to shape and angularity. At present, there is no excellent way to judge the state of the textural distribution of asphalt

pavement surface texture. Further development of evaluation metrics is needed to better predict pavement friction performance.

References

1. Zhang, J.; Li, C.; Ding, L.; Li, J. Performance evaluation of cement stabilized recycled mixture with recycled concrete aggregate and crushed brick. *Constr. Build. Mater.* 2021, 296, 123596.
2. Sun, Z.; Li, S.; Zhang, J.; Zeng, Y. Adhesion of Bituminous Crack Sealants to Aggregates Using Surface Energy Theory. *J. Mater. Civ. Eng.* 2020, 32, 04020299.
3. Yang, X.; Chen, S.; You, Z. 3D voxel-based approach to quantify aggregate angularity and surface texture. *J. Mater. Civ. Eng.* 2017, 29, 04017031.
4. Zhang, S.; Li, R.; Pei, J. Evaluation methods and indexes of morphological characteristics of coarse aggregates for road materials: A comprehensive review. *J. Traffic Transp. Eng. (Engl. Ed.)* 2019, 6, 256–272.
5. Li, J.; Zhang, J.; Qian, G.; Zheng, J.; Zhang, Y. Three-dimensional simulation of aggregate and asphalt mixture using parameterized shape and size gradation. *J. Mater. Civ. Eng.* 2019, 31, 04019004.
6. Masad, E.; Olcott, D.; White, T.; Tashman, L. Correlation of fine aggregate imaging shape indices with asphalt mixture performance. *Transp. Res. Rec.* 2001, 1757, 148–156.
7. Jun, Y.; Ye, Q. Morphological character of coarse aggregate and its influence on high-temperature shear strength of asphalt mixture. *J. Traffic Transp. Eng.* 2011, 11, 17–22.
8. Xiong, Q.; Wang, X.; Zhang, L. Research summary of digital image processing technology on coarse aggregate morphology characteristics. *Subgrade Eng.* 2012, 1, 7–10.
9. Wang, H.; Wang, D.; Liu, P.; Hu, J.; Schulze, C.; Oeser, M. Development of morphological properties of road surfacing aggregates during the polishing process. *Int. J. Pavement Eng.* 2017, 18, 367–380.
10. Singh, D.; Zaman, M.; Commuri, S. Comparison of shape parameters for selected coarse aggregates in Oklahoma. *J. Test. Eval.* 2012, 40, 409–426.
11. Wang, L.; Lane, D.S.; Lu, Y.; Druta, C. Portable image analysis system for characterizing aggregate morphology. *Transp. Res. Rec.* 2009, 2104, 3–11.
12. Al Rousan, T.M. Characterization of Aggregate Shape Properties Using a Computer Automated System; Texas A&M University: College Station, TX, USA, 2004.

13. Wang, A.; Zhang, Z.; Liu, K.; Xu, H.; Shi, L.; Sun, D. Coral aggregate concrete: Numerical description of physical, chemical and morphological properties of coral aggregate. *Cem. Concr. Compos.* 2019, 100, 25–34.
14. Miao, Y.; Yu, W.; Wu, J.; Wang, S.; Wang, L. Feasibility of one side 3-D scanning for characterizing aggregate shape. *Int. J. Pavement Res. Technol.* 2019, 12, 197–205.
15. Lucas Júnior, J.L.; Babadopulos, L.F.; Soares, J.B. Effect of aggregate shape properties and binder's adhesiveness to aggregate on results of compression and tension/compression tests on hot mix asphalt. *Mater. Struct.* 2020, 53, 43.
16. Mora, C.; Kwan, A. Sphericity, shape factor, and convexity measurement of coarse aggregate for concrete using digital image processing. *Cem. Concr. Res.* 2000, 30, 351–358.
17. Al-Rousan, T.; Masad, E.; Tutumluer, E.; Pan, T. Evaluation of image analysis techniques for quantifying aggregate shape characteristics. *Constr. Build. Mater.* 2007, 21, 978–990.
18. Komba, J.J.; Anochie-Boateng, J.K.; van der Merwe Steyn, W. Analytical and laser scanning techniques to determine shape properties of aggregates. *Transp. Res. Rec.* 2013, 2335, 60–71.
19. Anochie-Boateng, J.K.; Komba, J.J.; Mvelase, G.M. Three-dimensional laser scanning technique to quantify aggregate and ballast shape properties. *Constr. Build. Mater.* 2013, 43, 389–398.
20. Pan, T.; Tutumluer, E. Imaging-based direct measurement of aggregate surface area and its application in asphalt mixture design. *Int. J. Pavement Eng.* 2010, 11, 415–428.
21. Tutumluer, E.; Huang, H.; Hashash, Y.; Ghaboussi, J. Discrete element modeling of railroad ballast settlement. In *Proceedings of the AREMA Annual Conference, Chicago, IL, USA, 9–12 September 2007*.
22. Ge, H.; Sha, A.; Han, Z.; Xiong, X. Three-dimensional characterization of morphology and abrasion decay laws for coarse aggregates. *Constr. Build. Mater.* 2018, 188, 58–67.
23. Wadell, H. Sphericity and roundness of rock particles. *J. Geol.* 1933, 41, 310–331.
24. Mandelbrot, B.B.; Mandelbrot, B.B. *The Fractal Geometry of Nature*; WH Freeman: New York, NY, USA, 1982; Volume 1.
25. Lee, C.; Kramer, T.A. Prediction of three-dimensional fractal dimensions using the two-dimensional properties of fractal aggregates. *Adv. Colloid Interface Sci.* 2004, 112, 49–57.
26. Wang, L.; Wang, X.; Mohammad, L.; Abadie, C. Unified method to quantify aggregate shape angularity and texture using Fourier analysis. *J. Mater. Civ. Eng.* 2005, 17, 498–504.
27. Zhang, D.; Huang, X.; Zhao, Y. Investigation of the shape, size, angularity and surface texture properties of coarse aggregates. *Constr. Build. Mater.* 2012, 34, 330–336.

28. Rajan, B.; Singh, D. Understanding influence of crushers on shape characteristics of fine aggregates based on digital image and conventional techniques. *Constr. Build. Mater.* 2017, 150, 833–843.
29. Sun, W.; Wang, L.; Tutumluer, E. Image analysis technique for aggregate morphology analysis with two-dimensional Fourier transform method. *Transp. Res. Rec.* 2012, 2267, 3–13.
30. Moaveni, M.; Mahmoud, E.; Ortiz, E.M.; Tutumluer, E.; Beshears, S. Use of advanced aggregate imaging systems to evaluate aggregate resistance to breakage, abrasion, and polishing. *Transp. Res. Rec.* 2014, 2401, 1–10.
31. Wang, H.; Wang, C.; Bu, Y.; You, Z.; Yang, X.; Oeser, M. Correlate aggregate angularity characteristics to the skid resistance of asphalt pavement based on image analysis technology. *Constr. Build. Mater.* 2020, 242, 118150.
32. Kuo, C.Y.; Freeman, R.B. Imaging indices for quantification of shape, angularity, and surface texture of aggregates. *Transp. Res. Rec.* 2000, 1721, 57–65.
33. Isa, N.A.M.; Sani, Z.M.; Al-Batah, M.S. Automated Intelligent real-time system for aggregate classification. *Int. J. Miner. Process.* 2011, 100, 41–50.
34. Kuang, D.; Wang, X.; Jiao, Y.; Zhang, B.; Liu, Y.; Chen, H. Influence of angularity and roughness of coarse aggregates on asphalt mixture performance. *Constr. Build. Mater.* 2019, 200, 681–686.
35. Liu, P.; Hu, J.; Wang, D.; Oeser, M.; Alber, S.; Ressel, W.; Falla, G.C. Modelling and evaluation of aggregate morphology on asphalt compression behavior. *Constr. Build. Mater.* 2017, 133, 196–208.
36. Zhu, X.; Qian, G.; Yu, H.; Yao, D.; Shi, C.; Zhang, C. Evaluation of coarse aggregate movement and contact unbalanced force during asphalt mixture compaction process based on discrete element method. *Constr. Build. Mater.* 2022, 328, 127004.
37. Huang, B.; Chen, X.; Shu, X.; Masad, E.; Mahmoud, E. Effects of coarse aggregate angularity and asphalt binder on laboratory-measured permanent deformation properties of HMA. *Int. J. Pavement Eng.* 2009, 10, 19–28.
38. Miller, T.; Swiertz, D.; Tashman, L.; Tabatabaee, N.; Bahia, H.U. Characterization of asphalt pavement surface texture. *Transp. Res. Rec.* 2012, 2295, 19–26.
39. Al-Assi, M.; Kassem, E.; Nielsen, R. Using Close-Range Photogrammetry to Measure Pavement Texture Characteristics and Predict Pavement Friction. *Transp. Res. Rec.* 2020, 2674, 794–805.
40. Khasawneh, M.A.; Shbeeb, N.I.; Al-Omari, A.A. Analytical tool to shorten polishing time based on mean texture depth (MTD) of flexible pavements. *Road Mater. Pavement Des.* 2020, 21, 737–756.

41. Du, Y.; Weng, Z.; Li, F.; Ablat, G.; Wu, D.; Liu, C. A novel approach for pavement texture characterisation using 2D-wavelet decomposition. *Int. J. Pavement Eng.* 2022, 23, 1851–1866.
42. Hu, L.; Yun, D.; Liu, Z.; Du, S.; Zhang, Z.; Bao, Y. Effect of three-dimensional macrotexture characteristics on dynamic frictional coefficient of asphalt pavement surface. *Constr. Build. Mater.* 2016, 126, 720–729.
43. Cui, P.; Xiao, Y.; Yan, B.; Li, M.; Wu, S. Morphological characteristics of aggregates and their influence on the performance of asphalt mixture. *Constr. Build. Mater.* 2018, 186, 303–312.
44. Pan, T.; Tutumluer, E. Evaluation of visual based aggregate shape classifications using the University of Illinois Aggregate Image Analyzer (UIAIA). In *Pavement Mechanics and Performance*; American Society of Civil Engineers: Reston, VA, USA, 2006; pp. 203–211.
45. Singh, D.; Zaman, M.; Commuri, S. Inclusion of aggregate angularity, texture, and form in estimating dynamic modulus of asphalt mixes. *Road Mater. Pavement Des.* 2012, 13, 327–344.
46. Kutay, M.E.; Ozturk, H.I.; Abbas, A.R.; Hu, C. Comparison of 2D and 3D image-based aggregate morphological indices. *Int. J. Pavement Eng.* 2011, 12, 421–431.
47. Chen, J.S.; Hsieh, W.; Liao, M.C. Effect of Coarse Aggregate Shape on Engineering Properties of Stone Mastic Asphalt Applied to Airport Pavements. *Int. J. Pavement Res. Technol.* 2013, 6, 595–601.
48. Fletcher, T.; Chandan, C.; Masad, E.; Sivakumar, K. Measurement of aggregate texture and its influence on hot mix asphalt (HMA) permanent deformation. *J. Test. Eval.* 2002, 30, 524–531.
49. Maerz, N.H. Technical and computational aspects of the measurement of aggregate shape by digital image analysis. *J. Comput. Civ. Eng.* 2004, 18, 10–18.
50. Bessa, I.S.; Branco, V.T.C.; Soares, J.B.; Neto, J.A.N. Aggregate shape properties and their influence on the behavior of hot-mix asphalt. *J. Mater. Civ. Eng.* 2015, 27, 04014212.
51. Zhang, J.; Ding, L.; Li, F.; Peng, J. Recycled aggregates from construction and demolition wastes as alternative filling materials for highway subgrades in China. *J. Clean. Prod.* 2020, 255, 120223.
52. Aragão, F.T.S.; Pazos, A.R.G.; da Motta, L.M.G.; Kim, Y.R.; do Nascimento, L.A.H. Effects of morphological characteristics of aggregate particles on the mechanical behavior of bituminous paving mixtures. *Constr. Build. Mater.* 2016, 123, 444–453.
53. Wang, H.; Bu, Y.; Wang, Y.; Yang, X.; You, Z. The effect of morphological characteristic of coarse aggregates measured with fractal dimension on asphalt mixture's high-temperature performance. *Adv. Mater. Sci. Eng.* 2016, 2016, 6264317.
54. Puzzo, L.; Loprencipe, G.; Tozzo, C.; D'Andrea, A. Three-dimensional survey method of pavement texture using photographic equipment. *Measurement* 2017, 111, 146–157.

55. Grenfell, J.; Ahmad, N.; Liu, Y.; Apeagyei, A.; Large, D.; Airey, G. Assessing asphalt mixture moisture susceptibility through intrinsic adhesion, bitumen stripping and mechanical damage. *Road Mater. Pavement Des.* 2014, 15, 131–152.
 56. Cui, P.; Wu, S.; Xiao, Y.; Wang, F.; Wang, F. Quantitative evaluation of active based adhesion in Aggregate-Asphalt by digital image analysis. *J. Adhes. Sci. Technol.* 2019, 33, 1544–1557.
-

Retrieved from <https://encyclopedia.pub/entry/history/show/74989>